Materials Today Chemistry 17 (2020) 100301

Contents lists available at ScienceDirect

Materials Today Chemistry

journal homepage: www.journals.elsevier.com/materials-today-chemistry/

Needle-free electrospinning of nanofibrillated cellulose and graphene nanoplatelets based sustainable poly (butylene succinate) nanofibers

N. Neibolts [a], O. Platnieks [a], S. Gaidukovs [a, *], A. Barkane [a], V.K. Thakur [b], I. Filipova [c], G. Mihai [d], Z. Zelca [e], K. Yamaguchi [f], M. Enachescu [d, g]

[a] Faculty of Materials Science and Applied Chemistry, Institute of Polymer Materials, Riga Technical University, P.Valdena 3/7, Riga, LV, 1048, Latvia
[b] Biorefining and Advanced Materials Research Center, Scotland's Rural College (SRUC), Kings Buildings, Edinburgh, EH9 3JG, United Kingdom
[c] Latvian State Institute of Wood Chemistry, Latvia
[d] Center for Surface Science and Nanotechnology, University Politehnica of Bucharest, Romania
[e] Faculty of Materials Science and Applied Chemistry, Institute of Design Technologies, Riga Technical University, Latvia
[f] Graduate School of Integrated Science and Technology, Shizuoka University, 3-5-1 Johoku, Naka-ku, Hamamatsu 432-8561, Japan
[g] Academy of Romanian Scientists, 54 Spaiul Independentei, Bucharest, 050094, Romania

ARTICLE INFO

Article history:
Received 1 March 2020
Received in revised form
17 May 2020
Accepted 21 May 2020
Available online 20 June 2020

Keywords:
Needleless electrospinning
Bio-based polymer
Nanocellulose
3D Scaffolds
Theraml properties

ABSTRACT

Sustainable materials have slowly overtaken the nanofiber research field while the tailoring of their properties and the upscaling for industrial production are some of the major challenges. We report preparation of nanofibers that are bio-based and biodegradable prepared from poly (butylene succinate) (PBS) with the incorporation of nanofibrillated cellulose (NFC) and graphene nanoplatelets (GN). NFC and GN were combined as hybrid filler, which led to the improved morphological structure for electrospun nanofibers. A needleless approach was used for solution electrospinning fabrication of nanofiber mesh structures to promote application scalability. The polymer crystallization process was examined by differential scanning calorimetry (DSC), the thermal stability was evaluated by thermal gravimetric analysis (TGA), while the extensive investigation of the nanofibers structure was carried out with scanning electron microscopy (SEM) and atomic force microscopy (AFM). NFC and GN loadings were 0.5 and 1.0 wt %; while poly (ethylene glycol) (PEG) was employed as a compatibilizer to enhance fillers' interaction within the polymer matrix. The interactions in the interface of the fillers and matrix components were studied by FTIR and Raman spectroscopies. The hybrid filler approach proved to be most suitable for consistent and high-quality nanofiber production. The obtained dense mesh-based structures could have foreseeable potential application in biomedical field like scaffolds for the tissue and bone recovery, while other applications could focus on filtration technologies and smart sensors.

1. Introduction

The electrospinning process and nanofibers production process can be applied to many different polymer materials and tailored for a wide range of industries and applications [1,2]. Many possible advanced applications have been suggested such as water filtration, drug delivery, tissue engineering and materials for electronics [3]. Commonly used polymers for nanofiber preparation are fossil-based e.g. as polyethylene, polypropylene, poly(ethylene terephthalate), poly(vinyl alcohol), poly(ethylene glycol) [2]. However, global pollution problems have changed some of the requirements for future advanced materials considering the renewability and biodegradability of the used materials has become an essential feature to build sustainable products [4]. Bio-based polyesters are some of the best materials to replace oil-based polyolefins and polyesters in the production of electrospun nanofibers [5,6]. Poly(butylene succinate) (PBS) is an abundant bio-based polyester that is completely biodegradable and partly or fully produced from bio-based monomers [5,6]. PBS surpasses the other polyesters of polyhydroxyalkanoates (PHA) and polylactide (PLA) with mechanical properties that are comparable to polyethylene and polypropylene polymer materials [7]. PBS application for fiber electrospinning has been reported and discussed in the literature with various methods using its solution in organic solvents, compatible inorganic salts and needle electrospinning processing methods [8,9].

* Corresponding author.
E-mail address: sergejs.gaidukovs@rtu.lv (S. Gaidukovs).

https://doi.org/10.1016/j.mtchem.2020.100301
2468-5194/

The nanofiber application requires specific properties, like structural geometry, mechanical properties, porosity, size of pores, swelling capacity and water absorption, antibacterial properties and biodegradability and biocompatibility [10]. Rarely one single material can provide all of the required properties, that is why either polymer mixtures or additives are used [11]. Natural materials like cellulose, chitosan, alginate are all known for their ability to be compatible with water systems. The addition of the cellulose nanocrystals could enhance the stability of PVA electrospun fibers in water [12]. Cellulose is especially notable for mechanical strength that can provide additional structural support [10]. The mechanical strength and non-toxic nature of the cellulose make it suitable for the nanofiber production, but before that nanosized cellulose must be obtained such as nanofibrillated cellulose (NFC), which is obtained mainly by mechanical treatment compared to crystalline nanocellulose that require extensive chemical treatment [11]. Graphene and its various forms and modifications have gained great interest as an additive to the nanofibers. GN has a large surface area and it mixes well with various materials in powder forms, it can greatly affect porosity, increase the mechanical performance of the nanofibers and serve as a surface for antimicrobial particles or could even be used for drug release [13–15]. These and other chemical and physical properties make GN very suitable for the electrospinning process and preparation of the hybrid filler compositions. Synergy effects of the graphene-based hybrid fillers on the conductivity, thermal and mechanical properties are reported elsewhere [16,17].

It needs to be noted that two fundamentally different methods of electrospinning of polymer fibers are used nowadays, syringe needle method has been popular in the scientific community as easy and cheap set up for research purposes, but scaling and production introduce challenges thus needleless (needle-free) electrospinning has been proposed as an alternative [18]. The most commonly used needle type spinning is mainly based on mechanical forces and geometric boundary conditions (needle size and type). The second method, the needleless electrospinning, is based on the process of electrospun-induced fiber self-formation on an open surface electrode; its geometric shapes can be different [19]. The needleless approach has an upper hand since from the needle there can be only one Taylor cone that produces fibers while on open polymer bath electrospinning happens directly on the solution surface and various Taylor cones are occurring. The reduced needle electrospinning productivity can be improved by increasing the number of needles, but this type of process is accompanied by other drawbacks such as limited productivity increase, needle sticking, the need for a large work area, and so on [20].

Needleless electrospinning products morphology and dimension sizes can be controlled by controlling the humidity of the process, by choice of (bio)polymers, their concentrations, and combinations and by adjusting solution conductivity [19,21,22]. Higher humidity causes slower solvent evaporation, resulting in thinner fibers and as the conductivity is increased fiber diameter reduces as a result of the intensity increase of the Taylor cones formation [19,21]. Viscosity plays a major role in the electrospinning process and very high viscosities of polymer solutions can negate the possibility of fiber formation. In turn, when the viscosity of the polymer solution is too low the defects as droplets, beads, pores, and voids are usually introduced in nanofiber structure [2,23]. The solution viscosity is modified by changes in polymer concentration [9]. Inorganic salts and ionic liquids are used to control the charge density and surface tension of the solution [9]. Furthermore, some filler materials like poly(glycerol sebacate), poly(ethylene glycol) and poly(L-lactide) can be added to improve the electrospinning characteristics and overall quality of nanofibers [24–26]. Cellulose can be used to increase the viscosity of the solution [27] and NFC can decrease water vapor permeability in polymer blends [4]; while the carbon nanoparticles can enhance the electrical conductivity of the solution [28]. Thus, the synergetic use of several types of nanoscale fillers on the electrospinning conditions and composite nanofibers properties needs to be clarified.

The application of the fabricated PBS nanofiber meshes in the biomedical application as the scaffolds for the tissue and bone recovery relies on the biocompatibility of the polymer materials. The biodegradation and ecotoxicological studies on the microbial activity for nitrogen circulation activity has shown no adverse effects on the environment, presenting various application routes that involve material possible leakage [29]. No cytotoxicity has been observed for PBS, thus making it suitable for applications like scaffolds for tissue recovery and drug delivery [30]. These applications often need specific delivery routes and active particles on the surface. For example, the authors reported that natural amber particles loaded on the surface of the fiber materials provide enhanced medical fabric biocompatibility with skin cells [31]. The graphene incorporation has been also proposed as a biocompatible nanoparticle for fibers [14]. Potential for sensor technologies have been demonstrated using conductive graphene composite fibril nanostructures [32]. Implementation of highly active biopolymer porous mesh-structures that can facilitate active compounds for toxic waste treatment has been also suggested [33].

Our findings show potential for the application of the nanofibers in the biomedical and ecotechnology research field and give insights into the needleless method performance. The proposed idea of this study relates to the addition of NFC, GN and GN/NFC fillers to PBS polymer solution for electrospinning of composite nanofibers, fabrication of the nanofiber mesh-structures and the examination of their morphological appearance and properties. The electrospun fibers have been processed by needleless electrospinning. Since needle electrospinning of PBS composite nanofibers have prevailed in the scientific community as easy research set up [18], we believe this research on needless technology of the nanofiber fabrication could increase the overall productivity and benefit the industrial applications. The thermal properties and the morphology of the prepared nanofiber meshes were investigated for 6 different loadings of the NFC, GN and GN/NFC compared to pure PBS nanofibers.

2. Materials and methods

2.1. Materials

BioPBS™ FZ71PB® is a bio-based and biodegradable poly(-butylene succinate) (PBS) resin, produced by PTT MCC Biochem Company Ltd., that can be used for conventional thermoplastic extrusion, injection molding processing and industrial applications. PBS is characterized by density −1.36 g/cm^3, melt flow index MFI [190 °C, 2.16 kg] − 22 g/ 10min and melting point − 115 °C. Graphene (G3, 130 m^2/g, CAS = 7782-42-5) was purchased from Cambridge Nanosystems. Methanol (99,9%, Mw = 32,04%, CAS = 67-56-1) and chloroform (99,5%, Mw = 119,38%, CAS + 67-66-3) were purchased from Sigma−Aldrich. Poly(ethylene glycol) (PEG) (Honeywell Fluka, M_w = 285−315, CAS = 25322-68-3) was obtained from local distributor.

Nanofibrillated cellulose (NFC) was obtained from bleached birch hardwood Kraft pulp (kindly provided by Metsä Fibre, Finland) combining chemical treatment with ammonium persulfate and mechanical treatment with high shear laboratory mixer and reported in a previous study [34].

2.2. Characterizations

Differential scanning calorimetry (DSC) measurements were recorded for previously dried samples in a DSC-1 of Mettler Toledo (USA) under a nitrogen atmosphere. About 2 mg of composite samples were subjected to the whole DSC protocol, in which all the samples were heated to 150 °C at a rate of 10 °C/min, held at that temperature for 5 min and then cooled to 25 °C at a rate of 10 °C/min. The crystallization and melting temperatures, enthalpies, and crystallinities, respectively, were calculated from the experimental heating and cooling curves. Melting temperature (T_m) and the melting enthalpy (ΔH_m) were measured on the heating run, while crystallization temperature (T_c), was obtained from the cooling run. The crystallinity of the nanofibers was calculated using the following equation

$$\chi = \frac{\Delta H_m}{H_m^o\left(1 - W_f\right)} \times 100\% \quad (1)$$

where ΔH_m is the specimen's measured melting enthalpy, ΔH_m^o is the theoretical melting enthalpy of 100% crystalline PBS, the used value from literature 110.5 J/g [35] and W_f is the weight fraction of the fillers.

The thermogravimetric analysis (TGA) was performed with a Mettler TG50 instrument. Specimens about 3 mg in weight were heated from room temperature to 600 °C in the air atmosphere. The weight-loss heating curves and the differential weight-loss curves were used to study the material thermal stability. The weight loss calculation was processed as per the ASTM D3850 standard included in the Mettler original software.

Fungilab One rotational viscometer (Spain) was used to determine viscosity for prepared polymer solutions and WTW inoLabcond level 1 (US) was used for conductivity measurements.

FTIR-ATR was used to study the chemical bonds and interactions between the components of the prepared nanofibers. FTIR-ATR spectra of composites were collected at a resolution of 4 cm^{-1} on a Nicolet 6700 (ThermoScientific, Germany) in the region of 4000-800 cm^{-1}. Sixteen measurements of every specimen were performed, and the average spectrum is shown.

The room temperature Raman spectra of the samples were measured by Renishaw InVia90V727 micro-Raman spectrometer (UK) in the region of 200–1,900 cm^{-1} with a laser excitation wavelength of 514 nm, grading slit 1,800 nm^{-1}, power of 5% for exposure time 45 or 60 s and the number of accumulations was 5.

Hitachi SU 8230 Scanning Electron Microscope (Japan) was used to analyze the topography of the nanofibers. Secondary electron images were acquired at different magnifications using an accelerating voltage of 10 keV.

Atomic force microscopy (AFM) topography measurements were obtained with NTEGRA Spectra Probe NanoLaboratory developed by NT-MDT (Russia). The samples were prepared on the metal substrate and attached by scotch tape. The semicontact mode (Tapping mode) was selected which allows a maximum scannable measurement area of 100 μm × 100 μm and a maximum movement on the Z-axis of 7 μm. The cantilever NSG10 (single crystal silicon) with the resonance frequency of 240 kHz, the force constant of 11.8 N/m and the diameter of the tip about 6 nm was used to obtain results. Despite using the scotch tape, some fibers were floating on the substrate resulting in unstable topography.

3. Experimental

3.1. Fabrications of nanofibers

Nanofiber mesh materials preparation is summarized in Fig. 1. In the beaker, 100 g of NFC water suspension (2 wt%) was stirred at room temperature and 1 g of PEG was slowly added and homogenized for 20 min. After this, stirring was replaced with sonication using a probe-type ultrasonic homogenizer for 4 h. The solvent substitution was achieved by centrifugation and decantation followed by the addition of methanol and another sonication step, the process was repeated 3 times. The result of these processes yielded to 100 ml of PEG/NFC suspension in methanol (2 wt% of NFC).

Seven types of the nanofibers were electrospun and included the reference from pure PBS (abbreviated as PBS), two samples

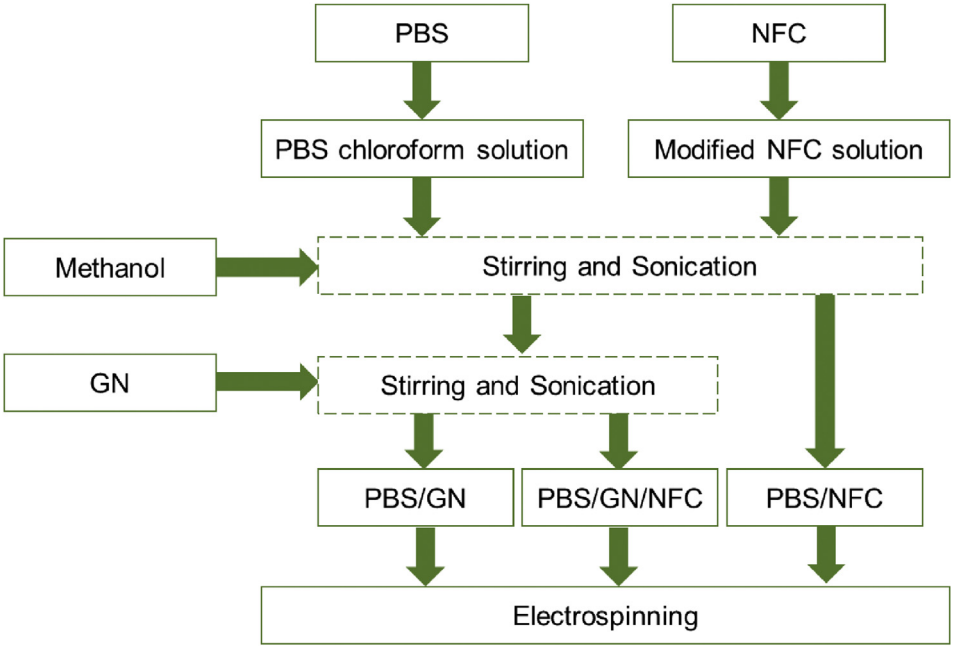

Fig. 1. Nanofiber preparation scheme.

consisted of 0.5 and 1.0 wt% graphene nanoplatelets (GN) and PBS (abbreviated as 0.5% GN and 1.0% GN), two specimens consisted of 0.5 and 1.0 wt% nanofibrillated cellulose (NFC) and PBS (abbreviated as 0.5% NFC and 1.0% NFC), and two hybrid compositions consisting of 0.5 wt % GN, 0.5 wt % NFC and 1.0 wt % GN, 1.0 NFC wt.% NFC (abbreviated as 0.5% GN/NFC and 1.0% GN/NFC).

Total mass for nanofiber solids was 12% w/v ratio with solvents and 80/20 chloroform and methanol v/v ratio for solvents were selected. A mass of 12 g PBS was dissolved in 80 ml chloroform and stirred for 3 h followed by the addition of 20 ml methanol from drop funnel. For the preparation of 0.5% NFC and 1% NFC nanofibers, in the first step, the PBS mass was reduced accordingly so that total mass of PBS and NFC is 12 g and previously prepared PEG/NFC suspension was diluted with methanol to 20 ml, which contained selected mass of NFC and added with drop funnel. To prepare 0.5% GN and 1.0% GN nanofibers total mass adjusted to 12 g and GN was added after the addition of methanol and sonication was applied for 1 h. For hybrid systems, both procedures were combined.

Table 1
Characteristics of prepared solutions.

Sample	μ, mPa·s	σ, μSv·cm^{-1}
PBS	35.9	4.51
0.5% GN	36.1	5.24
1.0% GN	36.4	6.25
0.5% NFC	58.7	4.59
1.0% NFC	83.6	4.62
0.5% GN/NFC	60.2	5.33
1.0% GN/NFC	84.0	6.22

The setup used in this study consisted of a Nanospider Lab 200 needle-free electrospinning equipment from Elmarco (Czech Republic). Pike spinning electrodes with 160 mm spinning distance, 15 kV spinning voltage were selected and the room temperature was 23 °C with relative humidity at 30%.

4. Results and discussion

4.1. Solution characteristics and nanofiber morphology

The obtained viscosity (μ) and conductivity (σ) values of the prepared solutions used for nanofibers electrospinning processing are summarized in Table 1. As was predicted, the addition of GN affects the conductivity of the investigated solution; NFC changes very strongly the viscosity of the solutions. For example, the sample 1.0% GN has shown an almost 1.4-fold increase in conductivity; while the sample 1.0% NFC has a 2-fold increase in viscosity. The transformation of the polymer solutions into nanofibers during electrospinning processing has been mainly guided by the used solution's properties of viscosity and conductivity [2]. Adjusted values of those parameters for every single solution composition have been beneficial for nanofibers with fewer defects and smaller diameters [36,37]. The simultaneous synergetic enhancement of conductivity and viscosity properties has been received for the solution compositions containing NFC and GN nanoparticles. The resulting PBS composite nanofiber materials have been examined by SEM. Different nanofiber morphologies are shown in Fig. 2, such as the one for the reference sample, PBS, (see Fig. 2a) in which defects in the shape of nodules can be observed. Fig. 2b, c shows the

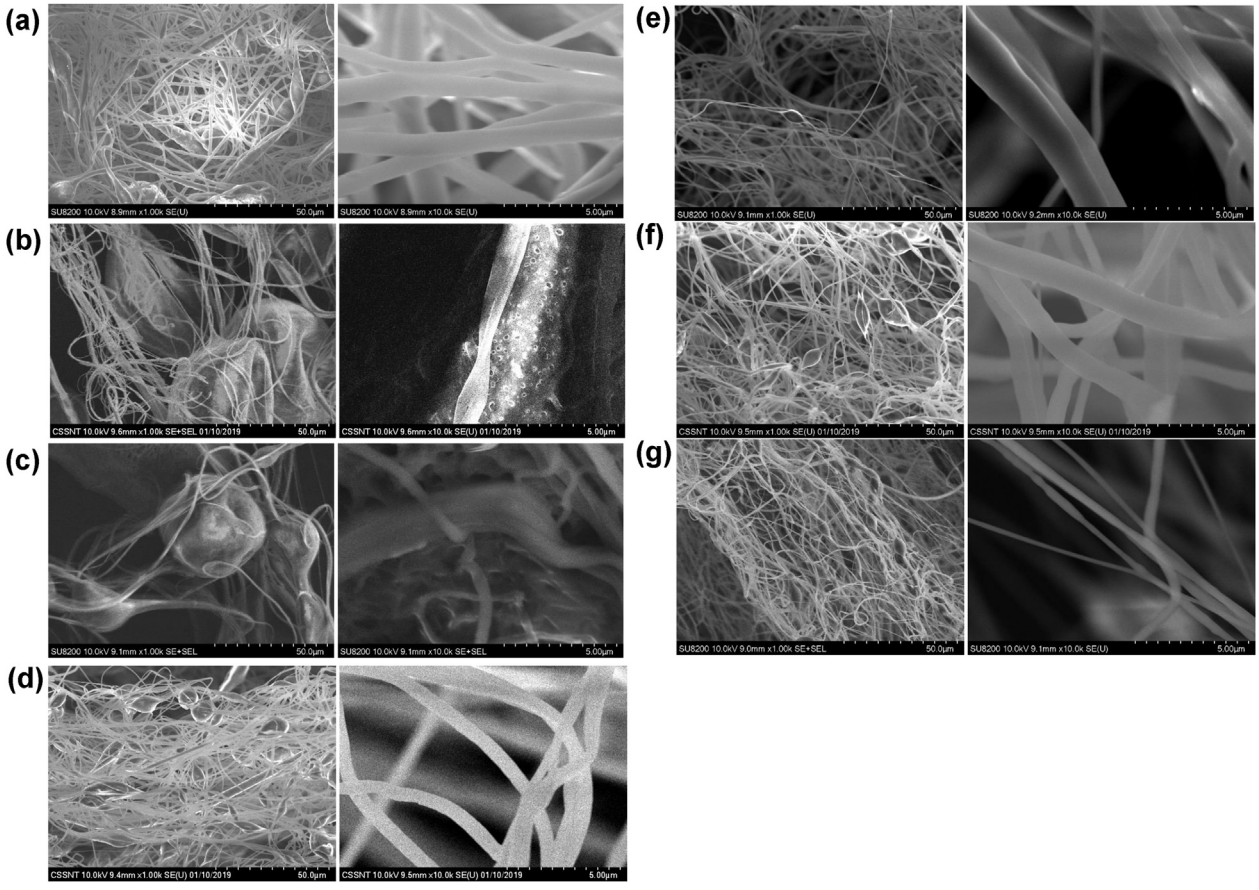

Fig. 2. SEM micrographs of obtained nanofiber: PBS (a), 0.5% GN (b), 1.0% GN (c), 0.5% NFC (d), 1.0% NFC (e), 0.5% GN/NFC (f), 1.0% GN/NFC (g).

morphology of the GN containing fibers that reveal big sphere-like agglomerations. The morphology of the hybrid samples is very similar to the one of the NFC samples as it can be observed in Fig. 2d–g. It has been found that 1.0% GN/NFC composition resulted in the highest solution viscosity, conductivity (Table 1) and fewer bead and void defects. It well corresponds to other authors' findings [38] that recognized that higher initial solution viscosity and conductivity strongly depressed the generation of defects such as beads and voids in the electrospun nanofibers. While neat PBS fibers and PBS composite fibers with incorporated GN and NFC nanoparticles contain obvious bead and void defects in their structure. The size of the beads decreased, while the shape of the beads transformed from spherical to the coil when the solution viscosity and conductivity enhanced after incorporation of nanoparticles. It should be also noted that in the investigated conditions range the defects have not completely disappeared. AFM topography measurements of these nanofibers are shown in Fig. 3. AFM also revealed the defects of the obtained electrospun fibers, while the size of the fibers is directly dependent on the composition. The resulting fibers have diameters in the range 200 nm - 1 μm. PBS has shown the fibers' average diameter of 1,000 nm, addition of 1.0% NFC took the diameter's sizes down to 700 nm. In turn, the incorporation of hybrid fillers 1.0% GN/NFC has decreased the average size down to 200 nm.

4.2. Thermal properties

The crystallinity (χ), the melting temperature (T_m) and the crystallization temperature (T_c) of the prepared composite fibers, calculated from the DSC heating and cooling thermograms (Fig. 4), are summarized in Table 2. As can be seen, the shape of the crystallization and melting transition peaks have been changed and shifted to a higher temperature range. This resulted from the transcrystallization behavior of the incorporated nanoparticles into the semicrystalline polymer matrix [39]. However, the crystallinity decreases from 69.1% for the PBS nanofiber to 64.9% and 59.6% for the samples 1.0% NFC and 1.0% GN correspondingly. The use of hybrid fillers 0.5% GN/NFC depressed the crystallinity to 58.7%, while, higher concentration 1.0% GN/NFC has a lower impact on the crystallinity that is equal to 64.5%. This observed aspect could be related to the nanoparticles' dispersion issues – their possible agglomeration at 1.0% concentration and consistent decrease of their specific contact area with the polymer matrix [39].

The melting temperature of PBS composite nanofibers remained almost unaffected and is equal to 114 °C for all composition samples. GN nanoparticles have not affected the crystallization and melting temperatures of the obtained materials. While NFC has a more pronounced influence on the crystallization temperature. It has been increased from 77.2 °C for sample PBS till 81.3 and 85.3 °C for samples containing 0.5% NFC and 1.0% NFC correspondingly. The crystallization temperature has the highest increase for the hybrid nanoparticles composition 1.0% GN/NFC, it is 7 °C higher than for the PBS nanofiber. The observed crystallization nucleating efficiency of the NFC nanoparticles over the GN nanoparticles could be characterized by their enhanced compatibility to the polymer that facilitates their dispersion within the polymer matrix, which was also reported in the literature [40]. Experimental data obtained by FTIR and Raman spectroscopy measurements have also evidenced some modification of the observed characteristic functional groups that can only correspond to the nanofiber composite materials filled with the NFC and the GN fillers.

The thermal stability of the nanofibers was tested with TGA. The weight loss and the differential weight characteristic curves are presented in Fig. 5. The form of TGA curves of the filled PBS composite and unfilled PBS has been found to be similar. Degradation

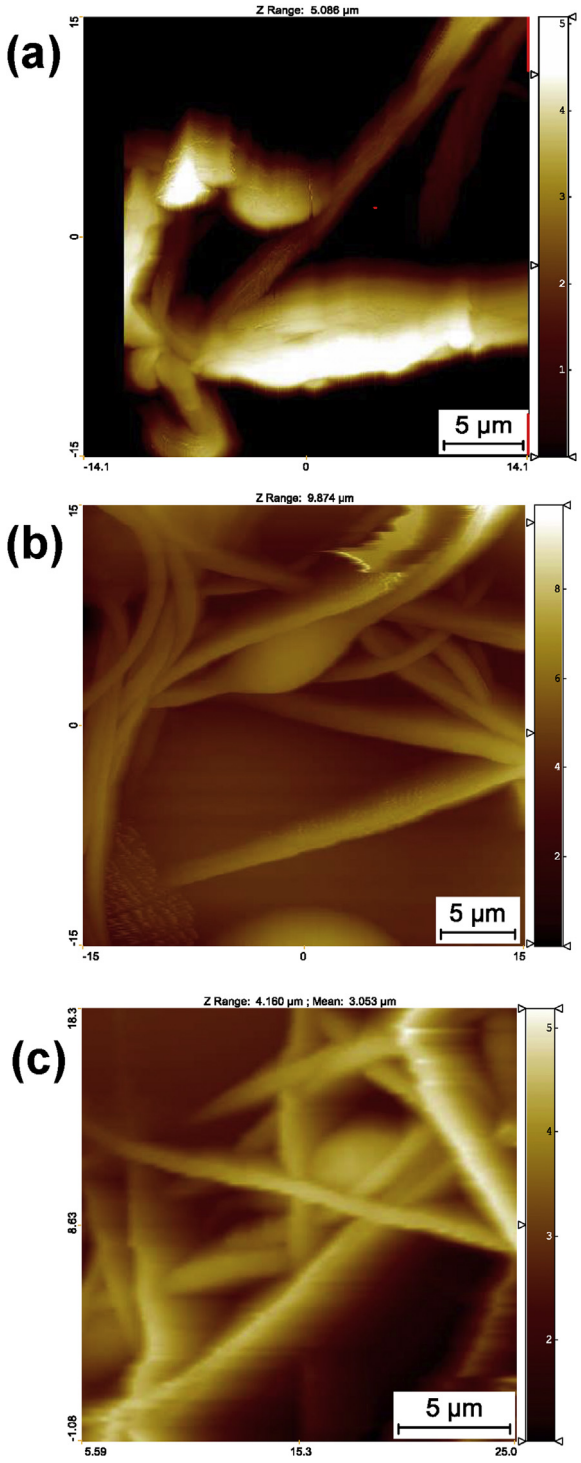

Fig. 3. AFM topography of PBS (a), 1.0% NFC (b) and 1.0% GN/NFC (c) nanofibers.

temperature T_{deg} that represents the temperature at the maximum weight loss rate is summarized in Table 2. The region from 50 to 125 °C shows small weight loss from around 0.1 to 0.5% this could be attributed to the evaporation of the water and the solvents from the nanofibers. More noticeable weight loss of the samples start to happen after 250 °C when specimens 1.0% NFC and 1.0% GN/NFC start to split from the other nanofiber curves. This could be explained with the presence of nanocellulose, which has lower

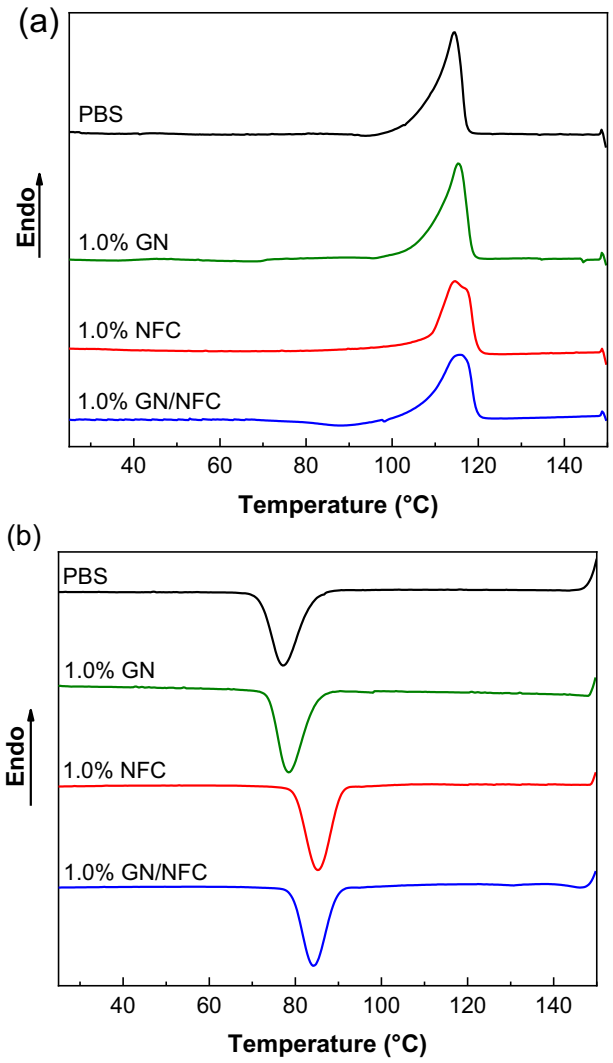

Fig. 4. DSC heating (a) and cooling (b) curves of nanofibers.

Table 2
Thermal properties of the prepared nanofibers.

Sample	T_{deg}	ΔH_m	χ, %	T_m, °C	T_c, °C
PBS	405	76.3	69.1	114.4	77.2
0.5% GN	400	66.2	60.2	115.1	78.2
1.0% GN	404	65.3	59.6	115.5	78.6
0.5% NFC	402	69.2	63.0	115.0	81.3
1.0% NFC	403	71.0	64.9	114.7	85.3
0.5% GN/NFC	400	64.2	58.7	115.2	82.0
1.0% GN/NFC	400	69.8	64.5	115.6	84.3

thermal stability compared to the PBS [41]. The differential weight loss curves show single-stage degradation that is characteristic for the PBS with degradation region from 325 to 425 °C approximately which is explained in the literature by a random cleavage of the ester bond [42]. The T_{deg} remained almost unaffected from the filler loading into the material, compared to the nanofibers obtained from unmodified PBS. T_{deg} was around 400–405 °C. Thus, no significant decrease in thermal stability was observed making both GN and NFC fillers suitable for applications together with PBS matrix. The PEG content in nanofibers is very small; the studies suggest that PEG remains stable to 250 °C temperature [43].

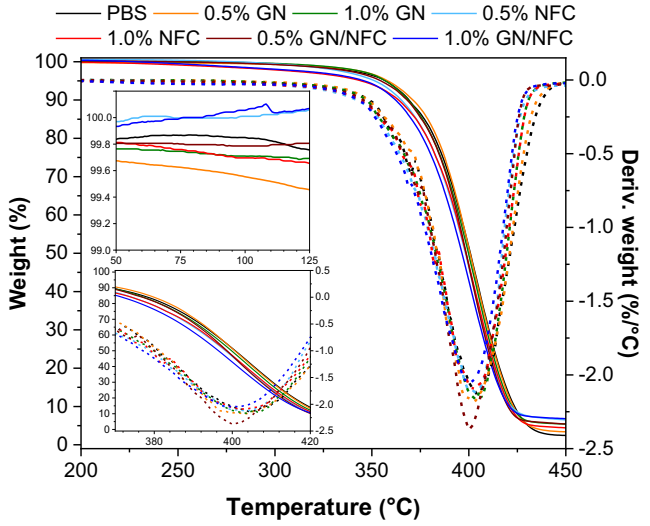

Fig. 5. TGA and DTG contours of the nanofibers under air atmosphere.

4.3. Spectral analysis

The obtained experimental FTIR and Raman spectra of the nanofiber samples are shown in Figs. 6 and 7 correspondingly. FTIR can be used to identify the PBS structure. The absorption bands at 2,946 cm^{-1} (1) and 1,330 cm^{-1} (3) corresponds to the methylene group CH_2 symmetric and asymmetric stretching vibrations [44,45]. The C=O stretching vibrations of the ester group is confirmed by the absorption band at 1,712 cm^{-1} (2) [27,28]. The band at 1,155 cm^{-1} (4) is related to C–O–C stretching vibrations and at 1,046 cm^{-1} (5) corresponding to the stretching vibrations O–C–C [45,46]. Remaining bands at 919 (6) an 806 cm^{-1} (7) are bending vibrations of C–OH from the carboxylic acid group [45].

The presence of graphene was verified by Raman spectroscopy because it can determine the hybridization state of carbon atoms. The absorption at 1,347 cm^{-1} corresponds to the D band which is defect-induced and confirms the presence of sp_3 carbon and 1,581 cm^{-1} to G band which is attributed to carbon sp_2 in-plane vibration [47,48]. Raman complements FTIR spectra and has many of the same bands as C–O–C (1), and C=O (3) with absorptions at 1,140 and 1,722 cm^{-1} but some absorptions are more pronounced

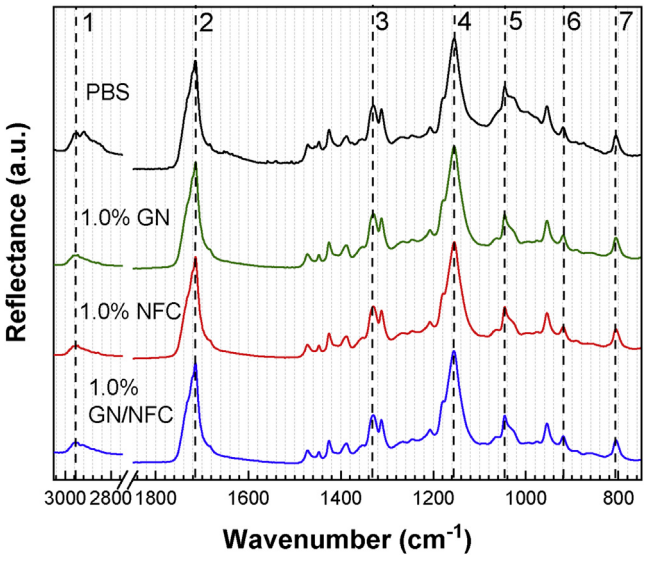

Fig. 6. FTIR spectra of obtained nanofibers.

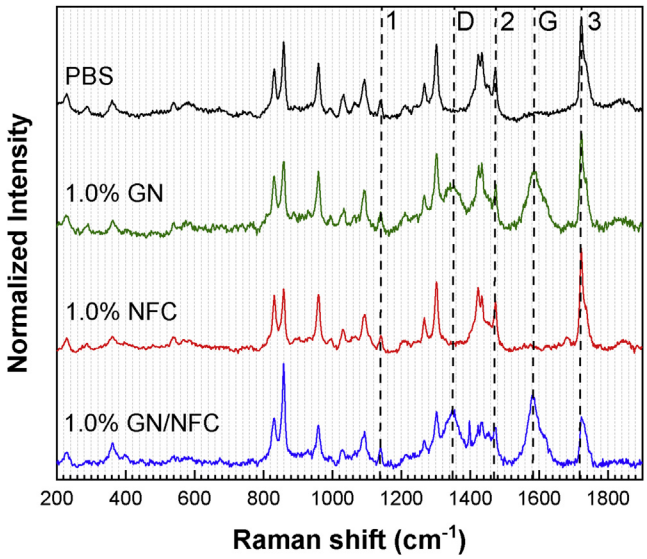

Fig. 7. RAMAN spectra of obtained nanofibers.

especially CH_2 (2) bend vibrations at 1,472 cm^{-1} [49–51]. No distinct cellulose absorptions were observed.

5. Conclusions

The proposed PBS electrospun nanofibers have been processed by needleless electrospinning technology. The incorporation of the nanofibrillated cellulose and graphene in the nanofibers resulted in enhanced properties arising from the synergic interactions of the nanoparticles during the electrospinning of the nanofibers. Therefore, the improved nanofiber mesh-structure quality was achieved by the fine-tuned solvent electrospinning process that has been facilitated by PEG compatibilization of nanoparticles and selection of the GN/NFC hybrid compositions. SEM testified that the use of the single NFC and GN nanoparticles has generated voids and beads defects on the nanofibers' surface. The thermal and crystallinity properties of the nanofiber materials were also dependent on the incorporated amount of NFC and GN. The thermal gravimetric investigations assured that the addition of these nanoparticles does not harm fabricated nanofibers mesh material's thermal stability.

The proposed needless technology of PBS nanofiber's fabrication would benefit productivity and industrial applications. The obtained mesh-based nanofiber material could be used in the biomedicine, filtration and smart sensors technologies.

Credit author statement

Nauris Neibolts: Conceptualization, Investigation. **Oskars Platnieks:** Conceptualization, Investigation, Writing - review & editing. **Sergejs Gaidukovs:** Conceptualization, Supervision, Writing - review & editing. **Anda Barkane:** Investigation, Writing - review & editing. **Vijay Kumar Thakur:** Supervision, Writing - review & editing. **Inese Filipova:** Investigation. **Geanina Mihai:** Investigation. **Zane Zelca:** Investigation. **Kensuke Yamaguchi:** Investigation. **Marius Enachescu:** Supervision, Writing - review & editing.

Funding sources

This research is funded by the Latvian Council of Science, project WOODMIMIC, project No. lzp-2018/1-0136. Romanian team would like to acknowledge the Romanian Ministry of Research and Innovation and by the European Union, under projects ECSEL-H2020 R3PowerUP project (Ctr. no. 1/1.1.3/31.01.2018, POC-SMIS code 115833), ECSEL-H2020 MADEin4 project (Ctr. no. 8/1.1.3H/06.01.2020, POC-SMIS code 128826) and ECSEL-H2020 OCEAN12 project (Ctr. no. 9/1.1.3H/20.01.2020, POC-SMIS code 129948).. This work was supported by the CA COST Action CA15107 - MultiComp (Multi-Functional Nano-Carbon Composite Materials Network).

Data availability

The raw/processed data required to reproduce these findings cannot be shared at this time as the data also forms part of an ongoing study.

Declaration of competing interest

The authors declare that they have no known competing financial interests or personal relationships that could have appeared to influence the work reported in this paper.

Acknowledgements

The authors wish to thank their parental institutes for providing the necessary facilities to accomplish this work.

References

[1] J.D. Schiffman, C.L. Schauer, A review: electrospinning of biopolymer nanofibers and their applications, Polym. Rev. 48 (2) (2008) 317, https://doi.org/10.1080/15583720802022182.
[2] Z.-M. Huang, Y.Z. Zhang, M. Kotaki, et al., A review on polymer nanofibers by electrospinning and their applications in nanocomposites, Compos. Sci. Technol. 63 (15) (2003) 2223, https://doi.org/10.1016/s0266-3538(03)00178-7.
[3] L. Persano, A. Camposeo, C. Tekmen, et al., Industrial upscaling of electrospinning and applications of polymer nanofibers: a review, Macromol. Mater. Eng. 298 (5) (2013) 504, https://doi.org/10.1002/mame.201200290.
[4] J.-W. Rhim, H.-M. Park, C.-S. Ha, Bio-nanocomposites for food packaging applications, Prog. Polym. Sci. 38 (10–11) (2013) 1629, https://doi.org/10.1016/j.progpolymsci.2013.05.008.
[5] P. Jambunathan, K. Zhang, Engineered biosynthesis of biodegradable polymers, J. Ind. Microbiol. Biotechnol. 43 (8) (2016) 1037, https://doi.org/10.1007/s10295-016-1785-z.
[6] G.Q. Chen, M.K. Patel, Plastics derived from biological sources: present and future: a technical and environmental review, Chem. Rev. 112 (4) (2012) 2082, https://doi.org/10.1021/cr200162d.
[7] P. Peças, H. Carvalho, H. Salman, et al., Natural fibre composites and their applications: a review, J. Compos. Sci. 2 (4) (2018), https://doi.org/10.3390/jcs2040066.
[8] E.H. Jeong, S.S. Im, J.H. Youk, Electrospinning and structural characterization of ultrafine poly(butylene succinate) fibers, Polymer 46 (23) (2005) 9538, https://doi.org/10.1016/j.polymer.2005.07.100.
[9] W. Klairutsamee, P. Supaphol, I. Jangchud, Electrospinnability of poly(butylene succinate): effects of solvents and organic salt on the fiber size and morphology, J. Appl. Polym. Sci. 132 (43) (2015), https://doi.org/10.1002/app.42716 n/a.
[10] R. Rasouli, A. Barhoum, M. Bechelany, et al., Nanofibers for biomedical and healthcare applications, Macromol. Biosci. 19 (2) (2019), e1800256, https://doi.org/10.1002/mabi.201800256.
[11] O. Nechyporchuk, M.N. Belgacem, J. Bras, Production of cellulose nanofibrils: a review of recent advances, Ind. Crop. Prod. 93 (2016) 2, https://doi.org/10.1016/j.indcrop.2016.02.016.
[12] A. Sutka, A. Sutka, S. Gaidukov, et al., Enhanced stability of PVA electrospun fibers in water by adding cellulose nanocrystals, Holzforschung 69 (6) (2015) 737, https://doi.org/10.1515/hf-2014-0277.
[13] E. Ceretti, P.S. Ginestra, M. Ghazinejad, et al., Electrospinning and characterization of polymer–graphene powder scaffolds, CIRP Ann. 66 (1) (2017) 233, https://doi.org/10.1016/j.cirp.2017.04.122.
[14] T. Arun, S.K. Verma, P.K. Panda, et al., Facile synthesized novel hybrid graphene oxide/cobalt ferrite magnetic nanoparticles based surface coating material inhibit bacterial secretion pathway for antibacterial effect, Mater. Sci. Eng. C Mater. Biol. Appl. 104 (2019) 109932, https://doi.org/10.1016/j.msec.2019.109932.
[15] S. De, S. Mohanty, S.K. Nayak, et al., Nanotoxicity of rare earth metal oxide anchored graphene nanohybrid: a facile synthesis and in vitro cellular

response studies, Nano 10 (6) (2015), https://doi.org/10.1142/s1793292015500915.
[16] P. Bertasius, J. Macutkevic, J. Banys, et al., Synergy effects in dielectric and thermal properties of layered ethylene vinyl acetate composites with carbon and Fe3O4 nanoparticles, J. Appl. Polym. Sci. 137 (24) (2020), https://doi.org/10.1002/app.48814.
[17] Y.S. Lee, Y.H. Park, K.H. Yoon, Flexural, electrical, thermal and electromagnetic interference shielding properties of xGnP and carbon nanotube filled epoxy hybrid nanocomposites, Carbon Lett. 24 (1) (2017) 41, https://doi.org/10.5714/CL.2017.24.041.
[18] M. Yu, R.-H. Dong, X. Yan, et al., Recent advances in needleless electrospinning of ultrathin fibers: from academia to industrial production, Macromol. Mater. Eng. 302 (7) (2017), https://doi.org/10.1002/mame.201700002.
[19] X. Zhang, K. Tang, X. Zheng, Electrospinning and crosslinking of COL/PVA nanofiber-microsphere containing salicylic acid for drug delivery, J. Bionic Eng. 13 (1) (2016) 143, https://doi.org/10.1016/s1672-6529(14)60168-2.
[20] Z. Zhu, P. Wu, Z. Wang, et al., Optimization of electric field uniformity of multi-needle electrospinning nozzle, AIP Adv. 9 (10) (2019), https://doi.org/10.1063/1.5111936.
[21] J. Pelipenko, J. Kristl, B. Jankovic, et al., The impact of relative humidity during electrospinning on the morphology and mechanical properties of nanofibers, Int. J. Pharm. 456 (1) (2013) 125, https://doi.org/10.1016/j.ijpharm.2013.07.078.
[22] N. Grimmelsmann, S.V. Homburg, A. Ehrmann, Needleless electrospinning of pure and blended chitosan, IOP Conf. Ser. Mater. Sci. Eng. 225 (2017), https://doi.org/10.1088/1757-899x/225/1/012098.
[23] A. Haider, S. Haider, I.-K. Kang, A comprehensive review summarizing the effect of electrospinning parameters and potential applications of nanofibers in biomedical and biotechnology, Arab. J. Chem. 11 (8) (2018) 1165, https://doi.org/10.1016/j.arabjc.2015.11.015.
[24] L. Liverani, A. Piegat, A. Niemczyk, et al., Electrospun fibers of poly(butylene succinate−co−dilinoleic succinate) and its blend with poly(glycerol sebacate) for soft tissue engineering applications, Eur. Polym. J. 81 (2016) 295, https://doi.org/10.1016/j.eurpolymj.2016.06.009.
[25] E. Llorens, H. Ibanez, L.J. Del Valle, et al., Biocompatibility and drug release behavior of scaffolds prepared by coaxial electrospinning of poly(butylene succinate) and polyethylene glycol, Mater. Sci. Eng. C Mater. Biol. Appl. 49 (2015) 472, https://doi.org/10.1016/j.msec.2015.01.039.
[26] N. Stoyanova, D. Paneva, R. Mincheva, et al., Poly(L-lactide) and poly(butylene succinate) immiscible blends: from electrospinning to biologically active materials, Mater. Sci. Eng. C Mater. Biol. Appl. 41 (2014) 119, https://doi.org/10.1016/j.msec.2014.04.043.
[27] H.P. Abdul Khalil, Y. Davoudpour, M.N. Islam, et al., Production and modification of nanofibrillated cellulose using various mechanical processes: a review, Carbohydr. Polym. 99 (2014) 649, https://doi.org/10.1016/j.carbpol.2013.08.069.
[28] G. Park, S. Kim, S. Chae, et al., Combining SWNT and graphene in polymer nanofibers: a route to unique carbon precursors for electrochemical capacitor electrodes, Langmuir 35 (8) (2019) 3077, https://doi.org/10.1021/acs.langmuir.8b03766.
[29] T.P. Haider, C. Volker, J. Kramm, et al., Plastics of the future? The impact of biodegradable polymers on the environment and on society, Angew Chem. Int. Ed. Engl. 58 (1) (2019) 50, https://doi.org/10.1002/anie.201805766.
[30] M. Gigli, M. Fabbri, N. Lotti, et al., Poly(butylene succinate)-based polyesters for biomedical applications: a review, Eur. Polym. J. 75 (2016) 431, https://doi.org/10.1016/j.eurpolymj.2016.01.016.
[31] S. Gaidukovs, I. Lyashenko, J. Rombovska, et al., Application of amber filler for production of novel polyamide composite fiber, Textil. Res. J. 86 (20) (2016) 2127, https://doi.org/10.1177/0040517515621130.
[32] K.M. Tripathi, F. Vincent, M. Castro, et al., Flax fibers – epoxy with embedded nanocomposite sensors to design lightweight smart bio-composites, Nanocomposites 2 (3) (2016) 125, https://doi.org/10.1080/20550324.2016.1227546.
[33] S.J. Park, G.S. Das, F. Schütt, et al., Visible-light photocatalysis by carbon-nano-onion-functionalized ZnO tetrapods: degradation of 2,4-dinitrophenol and a plant-model-based ecological assessment, NPG Asia Mater. 11 (1) (2019), https://doi.org/10.1038/s41427-019-0107-0.
[34] I. Filipova, V. Fridrihsone, U. Cabulis, et al., Synthesis of nanofibrillated cellulose by combined ammonium persulphate treatment with ultrasound and mechanical processing, Nanomaterials 8 (9) (2018), https://doi.org/10.3390/nano8090640.
[35] M.S. Nikolic, J. Djonlagic, Synthesis and characterization of biodegradablepoly(butylene succinate-co-butylene adipate)s, Polym. Degrad. Stabil. 74 (2001) 263, https://doi.org/10.1016/S0141-3910(01)00156-2.
[36] H. Fong, D.H. Reneker, Elastomeric nanofibers of styrene−butadiene−styrene triblock copolymer, J. Polym. Sci., Part B: Polym. Phys. 37 (1999) 3488.
[37] R. Jaeger, H. Schönherr, G.J. Vancso, Chain packing in electro-spun poly(-ethylene oxide) visualized by atomic force microscopy, Macromolecules 29 (1996) 7634.
[38] J.M. Deitzel, J. Kleinmeyer, D. Harris, et al., The effect of processing variables on the morphology of electrospun nanofibers and textiles, Polymer 42 (2001) 261.
[39] Y. Bin, H. Wang, in: T. Sabu, A.P. Mohammed, G.E. Bhoje, et al. (Eds.), Trans-crystallization in Polymer Composites and Nanocomposites, Crystallization in Multiphase Polymer Systems, Elsevier, Amsterdam, 2018.
[40] H.C. Bidsorkhi, A.G. D'Aloia, G. De Bellis, et al., Nucleation effect of unmodified graphene nanoplatelets on PVDF/GNP film composites, Mater. Today Commun. 11 (2017) 163, https://doi.org/10.1016/j.mtcomm.2017.04.001.
[41] G. Dorez, A. Taguet, L. Ferry, et al., Thermal and fire behavior of natural fibers/PBS biocomposites, Polym. Degrad. Stabil. 98 (1) (2013) 87, https://doi.org/10.1016/j.polymdegradstab.2012.10.026.
[42] K. Chrissafis, K.M. Paraskevopoulos, D.N. Bikiaris, Thermal degradation mechanism of poly(ethylene succinate) and poly(butylene succinate): comparative study, Thermochim. Acta 435 (2) (2005) 142, https://doi.org/10.1016/j.tca.2005.05.011.
[43] Y. Kou, S. Wang, J. Luo, et al., Thermal analysis and heat capacity study of polyethylene glycol (PEG) phase change materials for thermal energy storage applications, J. Chem. Therm. 128 (2019) 259, https://doi.org/10.1016/j.jct.2018.08.031.
[44] X. Hu, T. Su, W. Pan, et al., Difference in solid-state properties and enzymatic degradation of three kinds of poly(butylene succinate)/cellulose blends, RSC Adv. 7 (56) (2017) 35496, https://doi.org/10.1039/c7ra04972b.
[45] A. Gowman, T. Wang, A. Rodriguez-Uribe, et al., Bio-poly(butylene succinate) and its composites with grape pomace: mechanical performance and thermal properties, ACS Omega 3 (11) (2018) 15205, https://doi.org/10.1021/acsomega.8b01675.
[46] H.-S. Kim, H.-J. Kim, J.-W. Lee, et al., Biodegradability of bio-flour filled biodegradable poly(butylene succinate) bio-composites in natural and compost soil, Polym. Degrad. Stabil. 91 (5) (2006) 1117, https://doi.org/10.1016/j.polymdegradstab.2005.07.002.
[47] L. Liu, G. Huang, P. Song, et al., Converting industrial alkali lignin to biobased functional additives for improving fire behavior and smoke suppression of polybutylene succinate, ACS Sustain. Chem. Eng. 4 (9) (2016) 4732, https://doi.org/10.1021/acssuschemeng.6b00955.
[48] Z. Ni, Y. Wang, T. Yu, et al., Raman spectroscopy and imaging of graphene, Nano Res. 1 (4) (2010) 273, https://doi.org/10.1007/s12274-008-8036-1.
[49] S. Fischer, K. Schenzel, K. Fischer, et al., Applications of FT Raman spectroscopy and micro spectroscopy characterizing cellulose and cellulosic biomaterials, Macromol. Symp. 223 (1) (2005) 41, https://doi.org/10.1002/masy.200550503.
[50] M. Skrifvars, P. Niemelä, R. Koskinen, et al., Process cure monitoring of unsaturated polyester resins, vinyl ester resins, and gel coats by Raman spectroscopy, J. Appl. Polym. Sci. 93 (3) (2004) 1285, https://doi.org/10.1002/app.20584.
[51] C. Yanming, L. Jungang, F. Jimin, Spectral characterization of four kinds of biodegradable plastics: poly (lactic acid), poly (butylenes adipate-Co-terephthalate), poly (hydroxybutyrate-Co-hydroxyvalerate) and poly (butylenes succinate) with FTIR and Raman spectroscopy, J. Polym. Environ. 21 (1) (2012) 108, https://doi.org/10.1007/s10924-012-0534-2.